Journal of Power Sources 222 (2013) 45–51

Contents lists available at SciVerse ScienceDirect

Journal of Power Sources

journal homepage: www.elsevier.com/locate/jpowsour

Charge compensation mechanisms in $Li_{1.16}Ni_{0.15}Co_{0.19}Mn_{0.50}O_2$ positive electrode material for Li-ion batteries analyzed by a combination of hard and soft X-ray absorption near edge structure

Masatsugu Oishi [a,*], Takahiro Fujimoto [a], Yu Takanashi [a], Yuki Orikasa [b], Atsushi Kawamura [b], Toshiaki Ina [b], Hisao Yamashige [a], Daiko Takamatsu [a], Kenji Sato [a], Haruno Murayama [a], Hajime Tanida [a], Hajime Arai [a], Hideshi Ishii [c], Chihiro Yogi [c], Iwao Watanabe [c], Toshiaki Ohta [c], Atsushi Mineshige [d], Yoshiharu Uchimoto [b], Zempachi Ogumi [a]

[a] Office of Society-Academia Collaboration for Innovation, Kyoto University, Gokasho, Uji, Kyoto 611-0011, Japan
[b] Graduate School of Human and Environmental Studies, Kyoto University, Yoshida-Honmachi, Sakyo-ku, Kyoto 606-8501, Japan
[c] SR Center, Ritsumeikan University, 1-1-1 Noji-Higashi, Kusatsu, Shiga 525-8577, Japan
[d] Graduate School of Engineering, University of Hyogo, Himeji, Hyogo 671-2280, Japan

HIGHLIGHTS

- The redox reaction was studied by using hard and soft XANES spectroscopies.
- During the charge at a voltage plateau, some of the Ni and Co ions are reduced.
- We report the partial reduction of Ni and Co is associated with the ion migration.
- Soft XANES is effective to distinguish some of the surface specific reactions.

ARTICLE INFO

Article history:
Received 10 May 2012
Received in revised form
6 August 2012
Accepted 9 August 2012
Available online 28 August 2012

Keywords:
Li_2MnO_3
Lithium ion battery
In situ XAS
Positive material

ABSTRACT

The redox reaction of $Li_{1.16}Ni_{0.15}Co_{0.19}Mn_{0.50}O_2$ positive electrode material during the charging and discharging processes was investigated by using spectroscopic methods, i.e. *in situ* hard X-ray absorption near edge structure (XANES) at transition metal *K*-edges and *ex situ* soft XANES at oxygen *K*- and transition metal *L*-edges. The spectral changes of constituent elements during the initial charging to 4.5 V vs. Li/Li^+ are quite similar to those of conventional layer-structured positive materials, such as $LiNi_{1/3}Mn_{1/3}Co_{1/3}O_2$. Ni^{2+} and Co^{3+} ions are fully oxidized to Ni^{4+} and Co^{4+}, while Mn^{4+} remains unchanged. Ligand oxygen ions also take part in charge compensation. In the process of charging to 4.8 V via the plateau voltage region, no significant spectral change appears except partial reduction of Ni and Co ions in spite of lithium extraction. By discharging to 2.0 V the spectra of each element return to those of the pristine material.

1. Introduction

Layer-structured materials of $LiMO_2$, where M represents a transition metal element, have been conventionally used as the positive material in Li-ion batteries. The most commonly used material is $LiCoO_2$. Its theoretical capacity is 274 mAh g^{-1} when all the Li content is used. However, it is known that the extraction of Li ions from $LiCoO_2$ to form $Li_{1-x}CoO_2$ induces a phase transition from a hexagonal to a monoclinic system at the x value of 0.5 [1]. Therefore there is a limit of 0.5 to the de-lithiation depth x in order to obtain a rechargeable battery. The x value of 0.5 corresponds to a charge capacity of *ca.* 150 mAh g^{-1}.

In $LiMO_2$, M can be a mixture of several transition elements and $LiNi_{1/3}Co_{1/3}Mn_{1/3}O_2$ is used as an alternative material since its electrochemical and cycle properties are comparable or better than those of $LiCoO_2$ [2,3]. Due to the escalating demand for the higher-capacity Li-ion batteries, the usage of conventional materials has its

* Corresponding author. Tel.: +81 774 38 4968; fax: +81 774 38 4995.
E-mail addresses: m-ooishi@saci.kyoto-u.ac.jp, ooishi.masatsugu.6e@kyoto-u.ac.jp (M. Oishi).

0378-7753/$ – see front matter © 2012 Elsevier B.V. All rights reserved.
http://dx.doi.org/10.1016/j.jpowsour.2012.08.023

limits. One of the strategies in order to enhance the capacity is the use of higher Li content materials. Li_2MnO_3 is a layer-structured oxide whose formula can be written as $Li(Li_{1/3}Mn_{2/3})O_2$. It is one of the attractive candidates, as it possesses more Li ions per formula unit compared to the conventional layer-structured materials. The electrochemical properties of the Li rich positive electrode were first reported by Lu and Dahn [4]. They showed that $Li[Ni_xLi_{(1/3-2x/3)}Mn_{(2/3-x/3)}]O_2$ can cycle over 225 mAh g^{-1} between 2.0 and 4.8 V vs. Li/Li^+ with the reversible de-lithiation of almost one Li atom per formula unit. Moreover, Thackeray et al. have reported that more than one Li ion per formula unit can be extracted from a solid solution of Li_2MnO_3–$Li(Ni_{1/3}Co_{1/3}Mn_{1/3})O_2$. So that the material can be cycled at capacity as high as 280 mAh g^{-1} [5]. They concluded that during the charging process the Ni and Co ions were oxidized to compensate for the Li^+ extraction. With further Li^+ extraction at a high voltage, this material exhibits a distinctive electrochemical behavior, i.e. it shows a plateau voltage leading to a large irreversible capacity. The current–voltage profile for the first charging is totally different from the reversible profile after the first discharge. The first charging process involves an irreversible reaction. This leads to the rearrangement of the crystal structure and enables the Li-rich positive materials to de-lithiate at the capacity over 250 mAh g^{-1}. This is quite different from the conventional $LiMO_2$ materials, such as $LiNi_{1/3}Co_{1/3}Mn_{1/3}O_2$, in which a topotactic reaction proceeds from the first charging.

From the X-ray absorption spectroscopic (XAS) studies reported by many researchers [6–10], it is widely accepted that the transition metal ions are oxidized to their maximum, tetravalent state when they reach the plateau voltage region. Since the valence state remains unchanged during the plateau voltage region, something else must be oxidized [11,12]. Various studies have been reported concerning the mechanism of charge compensation during the de-lithiation reaction at that high voltage. Some groups suggested participation of the oxide ions at the high voltage and release of oxygen molecules as the charge compensation reaction [13,14]. However, it is also recognized that the amount of oxygen released from the positive electrode is too small to compensate all of the extra charge [6,7]. Thus, other mechanisms such as oxygen loss at the surface, densification of the crystal lattice and structural rearrangement caused by metal ion migration from surface to bulk have been considered [13].

In such a situation, in addition to hard XAS, soft XAS should be introduced to enhance our understanding about the redox reactions occurring in the metal oxides. The soft XAS spectra at both transition metal *L*-edge and O *K*-edge provide us with the knowledge of the charge distribution between the metal ion and ligand oxygen, since they are associated with the electronic transitions from corresponding core levels to hybridized orbitals of metal 3d and O 2p. Moreover, the soft XAS spectra can be obtained simultaneously in two different modes, a total electron yield (TEY) mode and a fluorescence yield (FY) mode. The former is surface sensitive, whose detection depth is less than 10 nm from the sample surface, while the latter is rather bulk sensitive with the depth of around 500 nm in the present study [15]. Compared to the hard XAS method, it is a great advantage of the soft XAS method that the characterization of surface and bulk of the metal oxide can be performed simultaneously on the same sample.

At present, most of the spectroscopic studies on the charge compensation mechanism in the redox reactions of metal oxides in batteries are performed using hard XAS. As described above, in addition to hard XAS, use of soft XAS should advance the present situation greatly. In this report, $Li(Li_{0.16}Ni_{0.15}Co_{0.19}Mn_{0.50})O_2$ as the positive electrode material is investigated using hard XAS and soft XAS both in TEY and FY modes for the first charge/discharge process and some of the results are compared to those of $Li(Ni_{1/3}Co_{1/3}Mn_{1/3})O_2$.

2. Experimental

2.1. Sample preparation

The powder of $Li_{1.16}Ni_{0.15}Co_{0.19}Mn_{0.50}O_2$ was prepared as follows. First, nitrate solutions each containing 2 mol dm^{-3} of metal ions in distilled water were prepared from $Ni(NO_3)_2{\cdot}6H_2O$(Wako, 99.9%), $Co(NO_3)_2{\cdot}6H_2O$ (Wako, 99.5%) and $Mn(NO_3)_2{\cdot}4H_2O$ (Fluka, 97.0 %UP). Desired quantities of metal nitrate solutions were added to a 2 mol dm^{-3} Na_2CO_3 aqueous solution. The pH of mixed solution was controlled between 7 and 8 during the precipitation process. The nickel–cobalt–manganese carbonate precipitate so produced was filtered, washed with distilled water, and dried over night at room temperature. The precipitate was mixed with $LiOH{\cdot}H_2O$ (Wako, 98–102%). 2 wt% excess $LiOH{\cdot}H_2O$ was used to offset any lithium evaporation loss during the next calcination process. The mixed powder was calcined at 1173 K for 12 h in air. The inductively-coupled plasma spectroscopy (ICP) analysis was conducted to determine the composition of the powders. Structural characterizations were performed by a powder X-ray diffraction method (XRD, Rigaku RINT2200) with Cu-$K\alpha$ (40 kV–40 mA). The XRD pattern confirmed that the obtained material was of a single phase without any obvious impurity phase.

2.2. Electrochemical characterization

Electrochemical characterization was performed using aluminum laminated cells. Positive electrodes were fabricated from mixtures containing 80 wt% of active material, 10 wt% of acetylene black (Denki Kagaku Kogyo Co.) as a conductive agent, and 10 wt% of polyvinylidene difluoride (Kureha Co.) as a binder. The total positive electrode loaded on the aluminum foil was 5.4 mg cm^{-2}. Lithium metal was used as the negative electrode and also as the reference electrode. The electrodes were separated by a porous polypropylene film. The electrolyte was 1 mol dm^{-3} $LiPF_6$ in ethylene carbonate/ethylmethyl carbonate (3:7 ratio by volume).

Fig. 1 shows the first charging and discharging profiles of the cell at a current density of 40 mA g^{-1} (a rate of 1/9 C) with the cut-off voltages of 2.0 and 4.8 V vs. Li/Li^+ at room temperature. A plateau voltage was observed at around 4.5 V in the first charging process and a large irreversible discharge capacity of 250 mAh g^{-1} was obtained. This charge and discharge profile is the same as the results of various studies reported by other groups [5,6,10].

The results of ICP elemental analysis are given in Table 1 for the positive electrodes which were charged by specified amounts. No transition metal elution during the charging process was detected by the ICP experiments. Excellent agreement found between the Li contents by the ICP analysis and those calculated from the charged capacity eliminates the possibility of decomposition of the

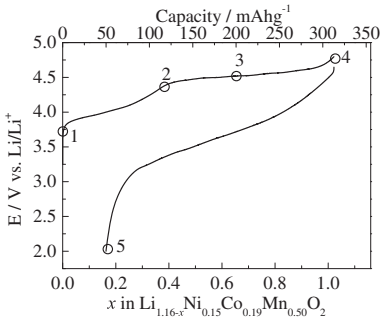

Fig. 1. First charge and discharge curves for $Li_{1.16}Ni_{0.15}Co_{0.19}Mn_{0.50}O_2$. The soft XAS measurements were carried out for the samples numbered 1 to 5 in the figure.

Table 1
Atomic ratios for $Li_{1.16}Ni_{0.15}Co_{0.19}Mn_{0.50}O_2$ during the first charging process determined by ICP analysis.

Charged capacity/mAh g^{-1}	Li[a]	Li	Mn	Ni	Co
0	1.16	1.156	0.507	0.129	0.208
100	0.82	0.808	0.506	0.131	0.207
200	0.49	0.489	0.506	0.132	0.206
300	0.17	0.178	0.507	0.131	0.206

[a] Calculated lithium contents assuming that all the current flow was used for de-lithiation.

electrolyte during the charging process. This fact proves that all the charge given to the electrode was used by the de-lithiation reaction of the positive material. For comparison, cells with $LiNi_{1/3}Co_{1/3}Mn_{1/3}O_2$ (Toda Kogyo Corporation, JAPAN) were also prepared.

2.3. X-ray absorption fine structure

The *in situ* hard XAS measurements at Ni, Co and Mn *K*-edges in a transmission mode were performed at the beam line BL14B2 of the synchrotron radiation facility SPring-8 (Hyogo, JAPAN). A Si(111) double crystal monochromator was used. The energy scale was calibrated using a Cu foil. In order to obtain *in situ* XAFS data of a reasonable quality, the amount of the electrolyte and thickness of the electrodes were adjusted appropriately. The XAS spectra was collected during the charging and discharging processes approximately at every 10% step of the fully charged state. Three XAS spectra of different *K*-edges were measured in the same *in situ* cell, at the open circuit voltage states after every charging step in order to observe the three spectra at the same electrochemical conditions.

The soft XAS data at O *K*- and metal *L*-edges were obtained at the beam line BL2 of Ritsumeikan University SR Center (Shiga, JAPAN) [16]. Results for five samples with different Li contents corresponding to the numbered points in Fig. 1 were electrochemically prepared using coin cells. In an argon filled glove box, the coin cells were disassembled to take out the samples of positive electrode material. They were rinsed with dimethyl carbonate to remove the electrolyte and dried. To avoid the exposure of the samples to the air, they were transferred to the high vacuum sample chamber of BL2 via a transfer vessel filled with argon gas [17]. The soft XAS data were obtained both in the partial FY (PFY) mode with a silicon drift detector (KETEK, VITUS R100 with a 0.1 μm Palylene-N film window) and in the TEY mode (the sample current mode), simultaneously. The spectrum of the different electrode parts was measured to get rid of the uncertainty by the areas on the electrode and check the reproducibility of the results.

3. Results

3.1. The hard X-ray absorption near edge structure

In situ XANES spectra at the Ni *K*-edge are shown in Fig. 2 (a) for $Li_{1.16-x}Ni_{0.15}Co_{0.19}Mn_{0.50}O_2$ samples with different Li contents, x during the first charging process. The spectra shifted to higher energy by charging up to the state, $x = 0.53$ and turned back to lower energy by further charging, as more clearly shown in the inset of Fig. 2(a). In Fig. 2(b), the *K*-edge energies are plotted as a function of x and those of $LiNi_{1/3}Co_{1/3}Mn_{1/3}O_2$ are included for comparison. The absorption energy shift reflects the variation of the electronic structure. During the charging process, the Li ions are extracted from the oxides. Generally, the Li^+ extraction leads to the increase in the valency of the transition metal ion to compensate the charge. In $LiNi_{1/3}Co_{1/3}Mn_{1/3}O_2$, the Ni *K*-edge absorption energy

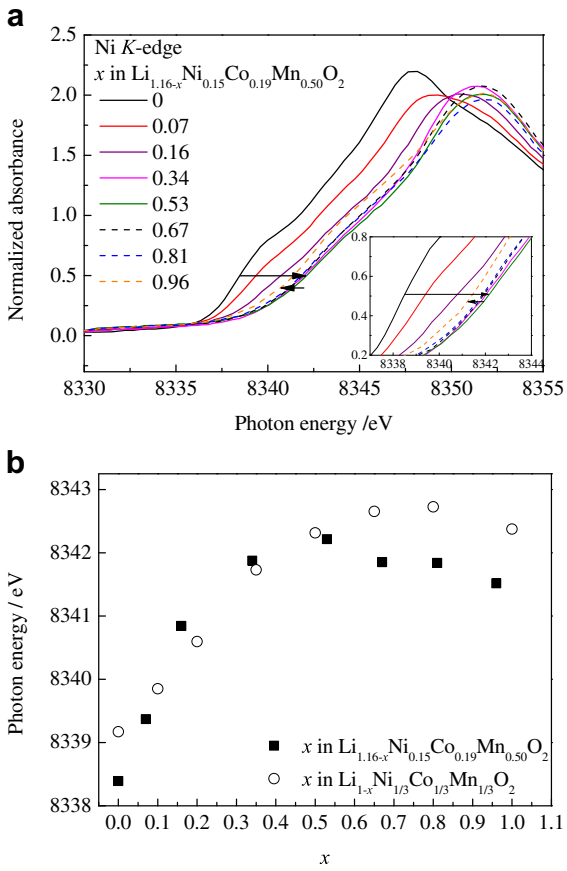

Fig. 2. (a) Ni *K*-edge XANES spectra of $Li_{1.16-x}Ni_{0.15}Co_{0.19}Mn_{0.50}O_2$ and (b) *K*-edge absorption energies of $Li_{1.16-x}Ni_{0.15}Co_{0.19}Mn_{0.50}O_2$ and $Li_{1-x}Ni_{1/3}Co_{1/3}Mn_{1/3}O_2$ as a function of Li content. The *K*-edge energies are evaluated at the absorbance of 0.5.

continues to increase up to the fully charged state as reported by Kim et al. [18], indicating that the oxidation of the Ni ions occurs continuously as the compensation reaction. In $Li_{1.16-x}Ni_{0.15}Co_{0.19}Mn_{0.50}O_2$, however, the Ni ions behave strangely, i.e. all of them are first oxidized but some are reduced by further Li extraction above $x = 0.53$.

XANES spectra at the Co *K*-edge obtained during the first charging are shown in Fig. 3. The absorption energy increased with charging. As reported by Kim et al. [19], the energy shift with the charging indicates that Co ions are also oxidized to compensate for the Li-ion extraction. It must be pointed out that the behavior of Co ions in terms of the dependence of absorption energy on Li-ion content is quite similar to those of the Ni ions, i.e. the valence state of Co in $Li_{1-x}Ni_{1/3}Co_{1/3}Mn_{1/3}O_2$ continuously increases until $x = 1$ but that of $Li_{1.16-x}Ni_{0.15}Co_{0.19}Mn_{0.50}O_2$ increases up to $x = 0.53$, then decreases.

The Mn *K*-edge spectra are given in Fig. 4. The Mn *K*-edge spectra change continuously with the charging with isosbestic points, indicating that the electronic structure does change, but the oxidation state of Mn ions stays unchanged [6–10,20]. The spectra exhibit a pre-edge absorption, which is assigned to a formally electric-dipole forbidden transition from 1s to 3d in an ideal octahedral symmetry, but appears by the 3d–4p orbital mixing caused by the distortion of MnO_6 octahedra.

Ito et al. studied the Mn *K* pre-edge spectra of the same system in detail [10]. They found a small shift (0.4 V) in the half-height energy between the fully charged and discharged states and related it to the Mn charge increase from 3.6+ to 4+ by full charge. Our results are similar to theirs, as shown in the inset of Fig. 4(a),

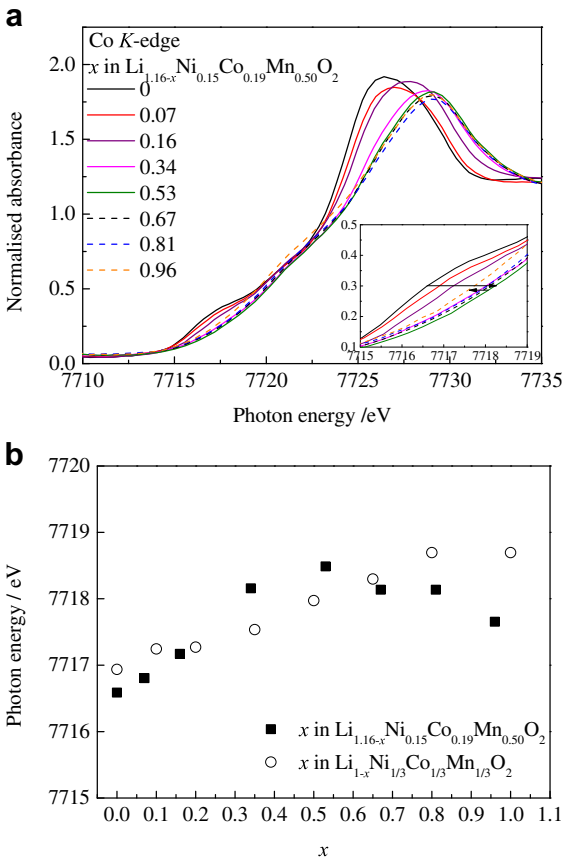

Fig. 3. (a) Co *K*-edge XANES spectra of $Li_{1.16-x}Ni_{0.15}Co_{0.19}Mn_{0.50}O_2$ and (b) *K*-edge absorption energies for $Li_{1.16-x}Ni_{0.15}Co_{0.19}Mn_{0.50}O_2$ and $Li_{1-x}Ni_{1/3}Co_{1/3}Mn_{1/3}O_2$ as a function of Li content. The *K*-edge energies are evaluated at the absorbance of 0.3.

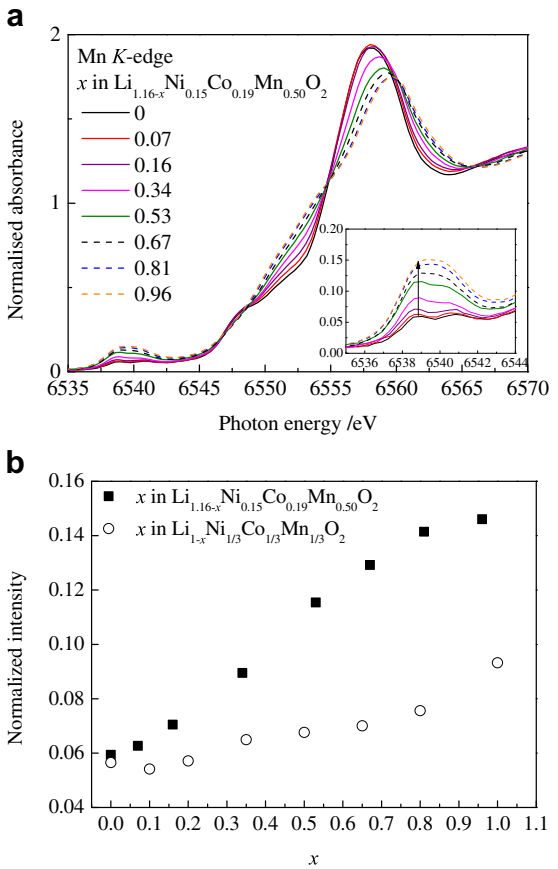

Fig. 4. (a) Mn *K*-edge XANES spectra of $Li_{1.16-x}Ni_{0.15}Co_{0.19}Mn_{0.50}O_2$ and (b) the intensities of the pre-edge peak evaluated at 6539 eV are compared for $Li_{1.16-x}Ni_{0.15}Co_{0.19}Mn_{0.50}O_2$ and $Li_{1-x}Ni_{1/3}Co_{1/3}Mn_{1/3}O_2$.

but we could not find a significant energy shift between the pristine and fully charged samples. Instead, the change in intensity of the pre-edge peak was significant. In Fig. 4 (b) the dependence of the pre-edge peak intensity at 6539 eV on the content of Li-ion, compared with that of $LiNi_{1/3}Co_{1/3}Mn_{1/3}O_2$ is given. The intensity for $Li_{1.16}Ni_{0.15}Co_{0.19}Mn_{0.50}O_2$ increased continuously with charging, indicating the enhancement of local structure distortion. In contrast, the pre-edge peak intensity of $LiNi_{1/3}Co_{1/3}Mn_{1/3}O_2$ has less dependence on the Li content, suggesting smaller structural change around Mn ions by charging.

3.2. The soft X-ray absorption near edge structure

In general, 3d transition metal *L*-edge XANES spectra are complicated due to the spin multiplicity both in the initial and final states. However, they provide direct information of unoccupied orbitals associated with oxidation state, spin state and bond covalency. Fig. 5 shows the Ni $L_{II,III}$-edge spectra taken both in TEY and PFY modes. The Ni L_{III} peak position before charging (spectrum 1) coincides with that of NiO (854.0 eV), indicating Ni ions exist mostly as Ni^{2+}. Drastic peak shift to 856 eV occurs by charging to 4.5 V as observed in both TEY and PFY spectra (spectrum 2). Ni L_{III} spectrum of NiO_2 obtained by electron energy loss spectroscopy [21] has a sharp peak at ~857 eV. The peak positions and profiles of the spectra at numbered points 2 and 3 are close and similar to those of NiO_2. Accordingly, Ni ions at the 4.5 V charging must be in Ni^{4+} state, or in a more strict sense, Ni^{4+} surrounded by oxygen ions. Similar results have been reported for $LiNi_{0.5}Mn_{0.5}O_2$ [22] and $LiNi_{1/3}Mn_{1/3}Co_{1/3}O_2$ [15,23]. However, compared with these spectra, the present ones show a more enhanced Ni L_{III} peak at 856.7 eV, which might be due to using a transfer vessel so as not to expose these samples to the air. Yoon et al. reported that the Partial EY (PEY) and FY spectra were quite different from each other [15,22], but they are almost identical in the present study. More careful observation of the spectra shown in Fig. 5(c) reveals a small contribution of Ni^{3+} and/or Ni^{2+} on the surface. However, we cannot exclude the possibility that the sample surface is reduced in the process of sample transfer via the transfer vessel.

Further charging up to 4.8 V (spectrum 4) generates a shoulder at the energy position of Ni^{2+} (854 eV), as shown in Fig. 5(c) and (d). This indicates further charging induces partial reduction of the Ni ions, as also suggested in the analysis of the Ni *K*-XANES spectra. By discharging (spectrum 5), the spectrum almost returns to that of the pristine sample (spectrum 1).

The Co *L*-edge XANES spectra are shown in Fig. 6. The profile and peak positions of the spectrum before charging (spectrum 1) are in good agreement with those of $LiCoO_2$, indicating Co ions exist as Co^{3+}. During the charging process, the spectra remain almost unchanged, but careful check reveals that the peak shifts to higher energy by 0.4 eV from step 1 to 3 and shifts back at step 4. The peak shift of the Co L_{III} edge in the chemically de-lithiated process has been studied for $LiCoO_2$ by Chen et al. [24]. They observed the peak shift of 0.6 eV by 35% de-lithiation, comparable with the charging to 4.5 V (spectrum 2), indicating that only small peak shift can be observed in the Co L_{III} edge spectra for the oxidation of Co^{3+} to Co^{4+}. Thus, the Co *L*-edge data can be understood in the same way as the Ni case.

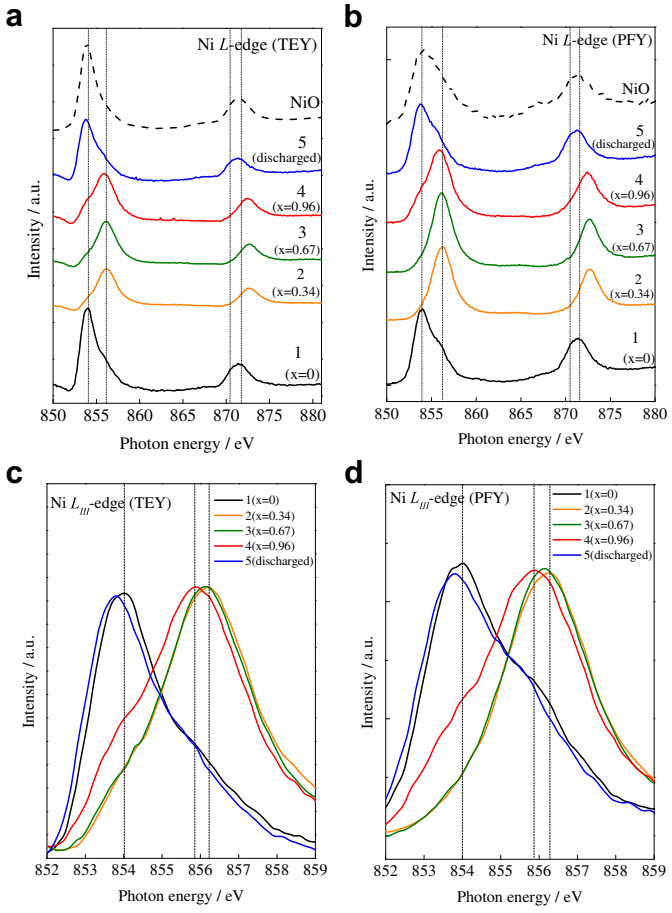

Fig. 5. The Ni *L*-edge XANES spectra of $Li_{1.16}Ni_{0.15}Co_{0.19}Mn_{0.50}O_2$ at numbered points indicated in Fig. 1 during the first charging/discharging process. They are obtained in (a)TEY and (b)PFY mode. The L_{III}-edge region is expanded in (c)TEY and (d)PFY. Note that the reference spectrum of NiO in the PFY mode was obtained by the inverse partial fluorescence yield mode [29] to avoid self absorption effects.

In general, Mn *L*-edge spectra change significantly depending on the oxidation state. The spectra shown in Fig. 7 are those of typical Mn^{4+} and essentially no peak shift was observed during the charging process. Thus, the Mn ions are not participating in the charge compensation process. The Mn L_{III}-edge spectrum of Mn^{4+} ion has a main peak at 643.2 eV and a sub-peak at 640.7 eV due to the spin multiplicity and the crystal field effect. Note that the TEY spectra in Fig. 7(a) show a decrease in the sub-peak intensity with charging, while almost no change is observed in the PFY spectra. This suggests that the charging induces the structural distortion around Mn ions at the oxide surface, but not in the bulk.

Fig. 8 shows the O *K*-edge XANES spectra, which provide information of the oxygen–metal interactions. The broad structures above 534 eV correspond to the transition of O 1s to the hybridized states consisting of metal 4sp and oxygen 2p orbitals (M_{4sp}–O_{2p}). The pre-edge structure below 534 eV corresponds to the transition to the states of M_{3d}–O_{2p} [15,26,27], which consists of a major peak at 529.5 eV and a sub-peak at 531 eV. The pre-edge structure of the spectrum before charging (spectrum 1) can be roughly explained by the superposition of O *K*-XANES peaks of Li_2MnO_3, $LiCoO_2$ and NiO in a molar ratio of 0.5:0.19:0.15.

The broad structures above 534 eV shifted to higher energy by charging up to 4.5 V. This corresponds to the oxidation of the Ni and Co ions observed in their *L*-edge spectra [15]. Two structures at 537 eV and 540 eV are assigned to the transition to σ^* (O–M), in

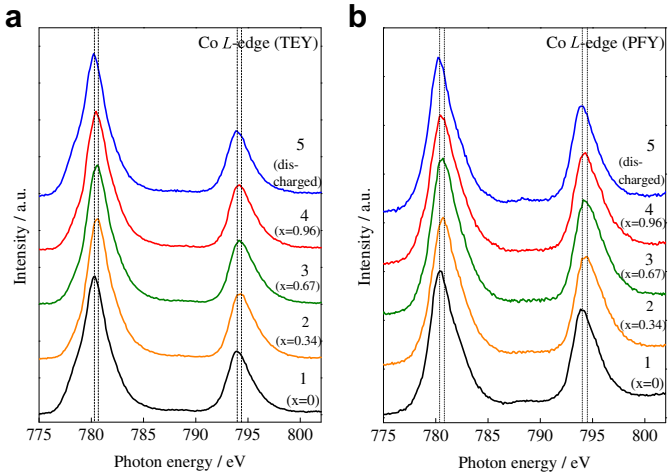

Fig. 6. Co *L*-edge XANES spectra of $Li_{1.16}Ni_{0.15}Co_{0.19}Mn_{0.50}O_2$ at numbered points indicated in Fig. 1 during the first charging and discharging process. They are obtained in (a)TEY and (b)PFY mode.

other words, 'shape resonance' [28]. The shift of these peaks to higher energy by charging reflects shortening of the bond distance due to the oxidation of metal ions to higher valency state [28].

The pre-edge region shows drastic changes upon charging, as shown in Fig. 8(c) and (d). The enhancement in integrated area over the pre-edge peak region is closely related to the charge compensation. In the lithium extraction process, electrons are removed from the Fermi level of the electrode which consists mainly of metal 3d orbitals. But due to the covalent bonding with oxygen, O 2p electrons are transferred to the metal ions to mitigate the charge. As a result, at the O 2p level more holes are created and the pre-edge peak gains in intensity. The pre-edge peak intensity is, therefore, a measure of the charge compensation of oxygen ions.

In the bulk of the electrode, i.e. from the PFY data, the pre-edge intensity increased by 20% by charging to 4.5 V, and did not increase by further charging, as shown in Fig. 8(d). This is comparable with the result for the de-lithiation of $LiNi_{1/3}Mn_{1/3}Co_{1/3}O_2$ reported by Yoon et al. [15]. Discharging recovered all the spectral features of

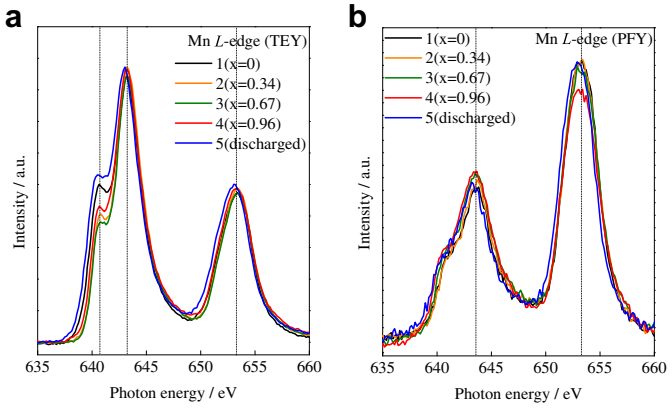

Fig. 7. The Mn *L*-edge XANES spectra of $Li_{1.16}Ni_{0.15}Co_{0.19}Mn_{0.50}O_2$ at numbered points indicated in Fig. 1 during the first charging and discharging process. They are obtained in (a)TEY and (b)PFY mode. Note that the Mn *L*-edge spectra in the TEY and PFY modes give quite different profiles. This is due to the fact that in the PFY mode, Mn L_{III}-edge peak is heavily suppressed by the presence of neighboring oxygen ions, which have the *K*-edge energy (543.1 eV) close to the Mn L_{III}-edge (638.7 eV) and absorb a fairly large amount of Mn $L\alpha$ emission [25].

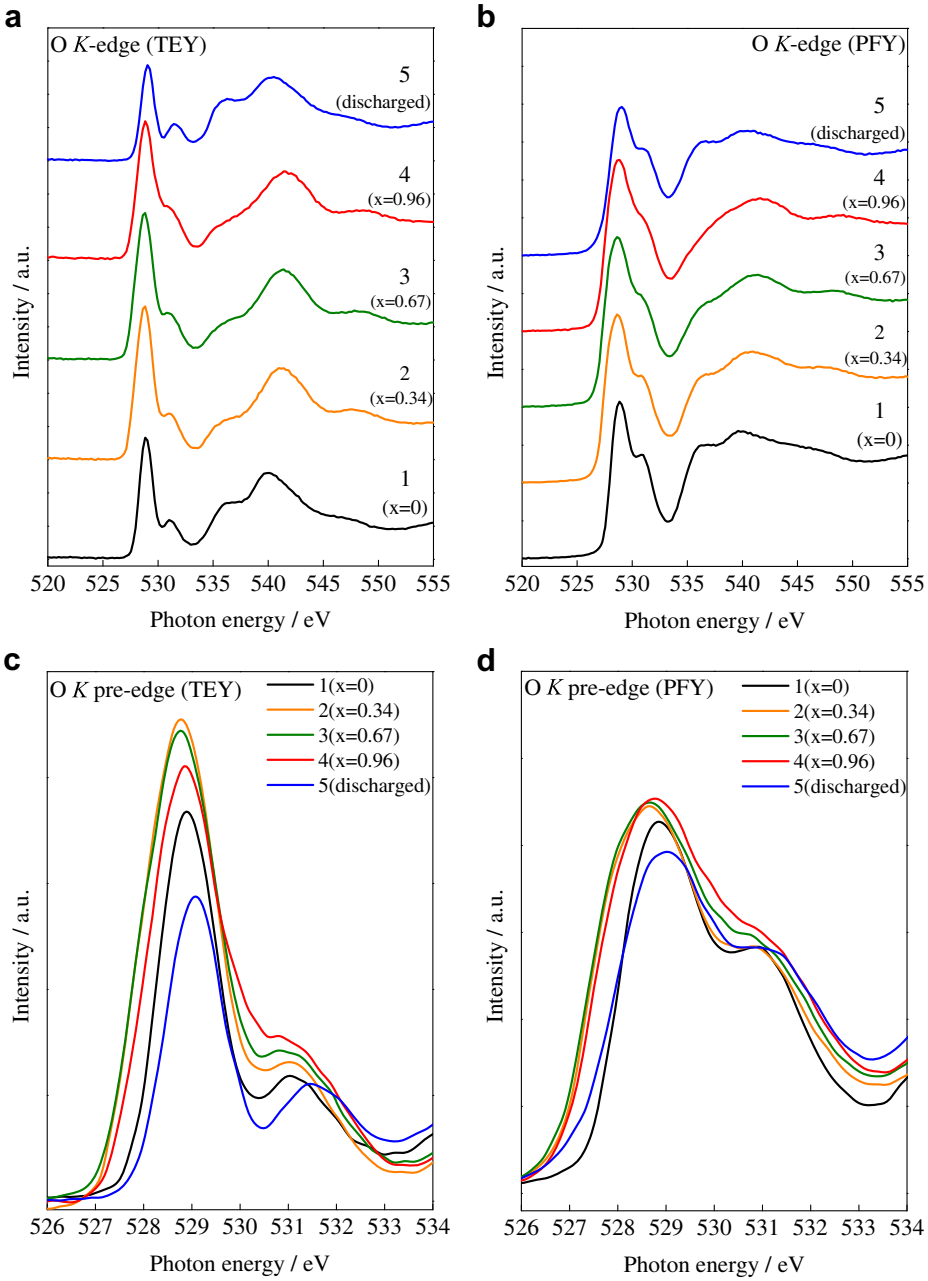

Fig. 8. O *K*-edge XANES spectra of $Li_{1.16}Ni_{0.15}Co_{0.19}Mn_{0.50}O_2$ at numbered points indicated in Fig. 1 during the first charging/discharging process. They are obtained in (a)TEY and (b) PFY mode. The pre-edge structures are expanded in (c)TEY and (d)PFY mode.

the pristine sample. In contrast to the PFY data, in PEY spectra, which is sensitive to the surface states of the electrode, the pre-edge intensity increased by 50% by charging to 4.5 V and decreased slightly from numbered point 3 to 4, as shown in Fig. 8(c). Discharging made it significantly smaller than that of the pristine sample. This result indicates that the surface of the electrode is more reduced than the bulk by the discharge process.

4. Discussion

The initial charge/discharge process can be roughly divided into three stages; (1) charging to 4.5 V, (2) further charging to 4.8 V after spanning a large plateau, and (3) discharging to 2.0 V. XANES spectra at Ni, Co, Mn *K*- and *L*-edges, and O *K*-edges provide information of the local structural change around each element during the process.

4.1. Charging to 4.5 V ($x = 0.53$)

Assuming the pristine $Li_{1.16-x}Ni_{0.15}Co_{0.19}Mn_{0.50}O_2$ consists of Li^+, Ni^{2+}, Co^{3+}, Mn^{4+} and O^{2-} ions and if all of the Ni^{2+} and Co^{3+} ions are oxidized to Ni^{4+} and Co^{4+}, respectively, the calculated amount of Li-ion extracted at the fully charged state corresponds to $x = 0.49$. This is in good agreement with $x = 0.53$, at which both the Ni and Co XANES adsorption peaks appeared at the highest energies.

Ni and Co *L*-edge spectra show that Ni^{2+} and Co^{3+} of the pristine sample change to fully oxidized Ni^{4+} and Co^{4+}, respectively, by

charging to 4.5 V. These results are supported by the corresponding *K*-edge spectra showing the edge shift to higher energy. In contrast, Mn valency remains unchanged as shown both in Mn *K*- and *L*-edge spectra. Instead, a structural distortion around the Mn ions occurs upon charging as indicated by the enhancement of the pre-edge peaks in Mn *K*-edge XANES. Spectral change suggests that distortions or structural changes takes place predominantly in the surface region. The pre-edge peak enhancement in the O *K*-XANES shows significant charge compensation by oxygen. These behaviors are almost the same as those of the conventional layered oxides, such as $LiNi_{1/3}Co_{1/3}Mn_{1/3}O_2$ [15].

4.2. Further charging from 4.5 V via the plateau voltage region

Unlike the conventional layered cathode materials, this system has a plateau voltage region in the charging process above 4.5 V. From the ICP results, it was confirmed that the Li ion extraction from the oxide still continued even after $x = 0.53$ all through to the charged state of 4.8 V. However, we could only observe a small edge-energy shift back to lower energy both in the Ni and Co *K*-edge spectra, indicating an apparent partial reduction of Ni^{4+} and Co^{4+} ions, as shown in Figs. 1(b) and 2(b). This behavior is also supported by the spectral changes in the *L*-edge data, as shown in Figs. 5 and 6. On the other hand, the pre-edge peak intensity in the O *K*-XANES of spectrum 4 was almost the same as that after charging to 4.5 V (spectrum 2), as shown in Fig. 8(c) and (d). This means that oxygen does not contribute to the charge compensation any more, even though Li ions are further extracted. To explain overall oxidation and the partial reduction of Ni and Co ions, some drastic structural changes should be considered, such as oxygen gas generation. Recently, Yabuuchi et al. confirmed by synchrotron X-ray diffraction that oxygen removal occurs and further claimed that it causes the Ni ion migration to lithium layers in the plateau voltage region [6]. Considering the similar ionic radii of Ni^{2+} (0.69 Å) and Li^+ (0.76 Å) for six-fold coordination, the movement of Ni^{2+} to the Li^+ vacancy must be energetically more favorable than that of Ni^{3+} or Ni^{4+}. Thus, the Ni ion migration into the lithium layer site is accelerated by reducing the Ni ion. Although present spectroscopic studies do not provide direct evidence of Ni ion migration, the reduction of Ni and Co ions might be related to the Ni and Co ion migration to the Li layer site.

4.3. Discharging to 2 V

By charging up to 4.8 V, some irreversible reactions occur and after discharging to 2 V the positive electrode material is not the same as the pristine material any more. The material after discharge was analyzed using Ni, Co, Mn *L*-edge and O *K*-edge XANES.

Ni, Co, and Mn *L*-edge spectra are almost the same as those of the pristine material, but a small difference is found in the O *K*-edge spectrum from that of the pristine one. Fig. 8(c) and (d) indicate that the intensity of the pre-edge peak of the discharged sample is lower than that of the pristine one, especially at the surface region. This means oxygen vacancies are more prevalent compared with the pristine state after a single charge/discharge cycle. This is in accordance with the mechanism of Ni ion reduction being more pronounced at the surface, as indicated in Fig. 5(c), where the peak intensity at 854 eV for spectra 2 and 3 are different.

5. Conclusion

The first charge/discharge process of the positive electrode material $Li_{1.16}Ni_{0.15}Co_{0.19}Mn_{0.50}O_2$ was studied and compared with that of $LiNi_{1/3}Co_{1/3}Mn_{1/3}O_2$ by using hard and soft XANES spectroscopies. Both spectroscopic techniques provided consistent data confirming that the following process take place, with the soft XANES experiments provided clearer evidence. During the charging process to 4.5 V, Ni and Co ions are oxidized to Ni^{4+} and Co^{4+}, respectively, while the Mn valency remains at 4+. After reaching 4.5 V, $Li_{1.16}Ni_{0.15}Co_{0.19}Mn_{0.50}O_2$ exhibits a flat voltage curve and at that voltage some of the Ni and Co ions are reduced even though the de-lithiation continues. The changes concerning the metal ion valency described above are supported by the O *K*-edge soft XANES experiments. The partial reduction of Ni and Co is most likely associated with the mechanism of Ni ion migration to the Li-ion layer site proposed by Yabuuchi et al. [6]. It is found that the surface sensitivity of soft XANES experiments is effective in distinguishing some of the surface specific reactions.

Acknowledgments

The authors thank Satoshi Yamahara, graduate student of University of Hyogo, for his help in carrying out the experiments. This work was supported by the Research and Development Initiative for Scientific Innovation of New Generation Batteries (RISING) project from New Energy and Industrial Technology Development Organization (NEDO) in Japan. The *in situ* XAS experiments in this study were carried out at Spring8 under proposals 2010B1032, 2010B1893, 2011A1010.

References

[1] J.N. Reimers, J.R. Dahn, J. Electrochem. Soc. 139 (8) (1992) 2091.
[2] T. Ohzuku, Y. Makimura, Chem. Lett. 642 (2001).
[3] N. Yabuuchi, T. Ohzuku, J. Power Sources 119–121 (2003) 171.
[4] Z. Lu, J.R. Dahn, J. Electrochem. Soc. 149 (7) (2002) A815.
[5] M.M. Thackeray, S.H. Kang, C.S. Johnson, J.T. Vaughey, R. Benedek, S.A. Hackney, J. Mater. Chem. 17 (2007) 3112.
[6] N. Yabuuchi, K. Yoshii, S.T. Myung, I. Nakai, S. Komaba, J. Am. Chem. Soc. 133 (12) (2011) 4404.
[7] Y.S. Hong, Y.J. Park, K.S. Ryu, S.H. Chang, M.G. Kim, J. Mater. Chem. 14 (2004) 1424.
[8] N. Tran, L. Croguennec, N. Tran, L. Croguennec, M. Menetrier, F. Weill, Ph .Biensan, C. Jordy, C. Delmas, Chem. Mater. 20 (2008) 4815.
[9] D.Y.W. Yu, K. Yanagida, Y. Kato, H. Nakamura, J. Electrochem. Soc. 156 (6) (2009) A417.
[10] A. Ito, Y. Sato, T. Sanada, M. Hatano, H. Horie, Y. Ohsawa, J. Power Sources 196 (2011) 6828.
[11] A.D. Robertson, P.G. Bruce, Chem. Mater. 15 (1984) 2003.
[12] B. Ammundsen, J. Paulsen, J. Adv. Mater. 13 (2001) 943.
[13] A.R. Armstrong, M. Holzapfel, P. Novak, C.S. Johnson, S.H. Kang, M.M. Thackeray, P.G. Bruce, J. Am. Chem. Soc. 128 (2006) 8694.
[14] Y. Koyama, I. Tanaka, M. Nagao, R. Kanno, J. Power Sources 189 (2009) 798.
[15] W.S. Yoon, M. Balasubramanian, K.Y. Chung, X.Q. Yang, J. McBreen, C.P. Grey, D.A. Fischer, J. Am. Chem. Soc. 127 (2005) 17479.
[16] H. Ishii, K. Nakanishi, I. Watanabe, T. Ohta, K. Kojima, e-J. Surf. Sci. Nanotechnol. 9 (2011) 416.
[17] K. Nakanishi, T. Ohta, in: Z. Haq (Ed.), Advanced Topics in Measurements, InTech, Croatia, 2012, p. 43.
[18] M.G. Kim, H.J. Shin, J.H. Kim, S.H. Park, Y.K. Sun, J. Electrochem. Soc. 152 (2) (2005) A1320.
[19] M.G. Kim, C.H. Yo, J. Phys. Chem. B 103 (1999) 6457.
[20] Y.W. Tsai, B.J. Hwang, G. Ceder, H.S. Sheu, D.G. Liu, J.F. Lee, Chem. Mater. 17 (2005) 3191.
[21] Y. Koyama, T. Mizoguchi, H. Ikeno, I. Tanaka, J. Phys. Chem. B 109 (2005) 10749.
[22] W.S. Yoon, M. Balasubramanian, X.Q. Yang, Z. Fu, D.A. Fischer, J.M. McBreen, J. Electrochem. Soc. 151 (2004) A246.
[23] H. Kobayashi, Y. Arachi, S. Emura, H. Kageyama, K. Tatsumi, T. Kamiyama, J. Power Sources 146 (2005) 640.
[24] C.H. Chen, B.J. Hwang, C.Y. Chen, S.K. Hu, J.M. Chen, H.S. Sheu, J.F. Lee, J. Power Sources 174 (2007) 938.
[25] Y. Tamenori, M. Morita, T. Nakamura, J. Synchrotron. Radiat. 18 (2011) 747.
[26] J. Graetz, A. Hightower, C.C. Ahn, R. Yazami, P. Rez, B. Fultz, J. Phys. Chem. B 106 (2002) 1286.
[27] Y. Uchimoto, H. Sawada, T. Yao, J. Power Sources 97-98 (2000) 326.
[28] J. Stöhr, NEXAFS Spectroscopy, Springer-Verlarg, Berlin, 1992.
[29] A.J. Achkar, T.Z. Regier, H. Wadati, Y.-J. Kim, H. Zhang, D.G. Hawthorn, Phys. Rev. B 83 (2011) 081106R.